

## New Triphenylamine-Based Dyes for Dye-Sensitized Solar Cells

Wei Xu, Bo Peng, Jun Chen,\* Mao Liang, and Fengshi Cai

*Institute of New Energy Material Chemistry and Engineering Research Center of Energy Storage and Conversion (Ministry of Education), College of Chemistry, Nankai University, Tianjin 300071, People's Republic of China*

*Received: August 31, 2007; In Final Form: October 20, 2007*

A series of new conjugated metal-free organic dyes (TC1, TC2, TC3, and TC4) comprising triphenylamine (TPA) moieties as the electron donor and cyanoacetic acid moieties as the electron acceptor/anchoring groups were designed at the molecular level and developed for the use in dye-sensitized solar cells (DSCs). Quantum chemical calculations have been performed to gain insight into structural, electronic, and optical properties of the as-synthesized sensitizers. The time-dependent density functional theory calculations allowed assignment of the experimental spectroscopic data. It is found that the photovoltaic performance of the DSCs with the as-synthesized dyes can be improved by enhancing the electron-donor ability and extending the  $\pi$ -conjugated bridge of the dyes. In particular, the DSCs based on 2-cyano-5-(4-(phenyl(4-vinylphenyl)amino)phenyl) penta-2,4-dienoic acid dye (TC4) showed an open circuit voltage of 652 mV, a short circuit photocurrent density of 11.5 mA cm<sup>-2</sup>, and a fill factor of 0.64, corresponding to an overall light to electricity conversion efficiency of 4.82% under AM 1.5 irradiation (100 mW cm<sup>-2</sup>). This result reveals that efficient electron injection from the excited sensitizer to the conduction band of titania film occurs, owing to the more delocalizing electrons of the bridge and donor part of the dyes.

### Introduction

Dye-sensitized solar cells (DSCs) demonstrated by Grätzel's group have attracted considerable interest for the conversion of sunlight to electricity.<sup>1</sup> There are four main factors that affect the performance of the DSCs: anode,<sup>2</sup> cathode,<sup>3</sup> electrolyte,<sup>4</sup> and photosensitive dyes.<sup>5</sup> As a key part of DSCs, the dyes take the function of light absorption and injection of the photoexcited electrons to the conduction band of the semiconductor in the anode. There have been two kinds of dyes, namely, metal-organic complexes and metal-free organic dyes, that have been summarized in Uchida's website.<sup>6</sup> Up to now, polypyridyl ruthenium(II) complex-based dyes<sup>7</sup> have exhibited conversion efficiencies over 10% for solar power to electricity in the standard DSCs with an I<sup>-</sup>/I<sub>3</sub><sup>-</sup> solution electrolyte, owing to their broad metal-to-ligand charge-transfer (MLCT) absorption bands, chemical stability of photoexcited states, and oxidized form.<sup>8</sup> In the meantime, alternative metal-free organic dyes, which generally possess larger molar extinction coefficients due to intramolecular  $\pi$ - $\pi^*$  transitions and can be designed more easily and economically, have shown the conversion efficiencies up to 8%.<sup>9–18</sup> Among the metal-free organic dyes, triphenylamine (TPA) and its derivatives as donor units have displayed promising properties in the development of photovoltaic devices.<sup>19–21</sup> Theoretical and experimental studies have demonstrated that TPA unit, which suppresses the dye aggregation for its nonplanar structure, can be used as the sensitizer of DSCs.<sup>22</sup> Recently, a few groups<sup>23–26</sup> have reported that DSCs with various triphenylamine-based dyes have shown the power conversion efficiencies of 3.5 to 5.8% under AM 1.5 irradiation, indicating the importance of their further investigation in DSCs.

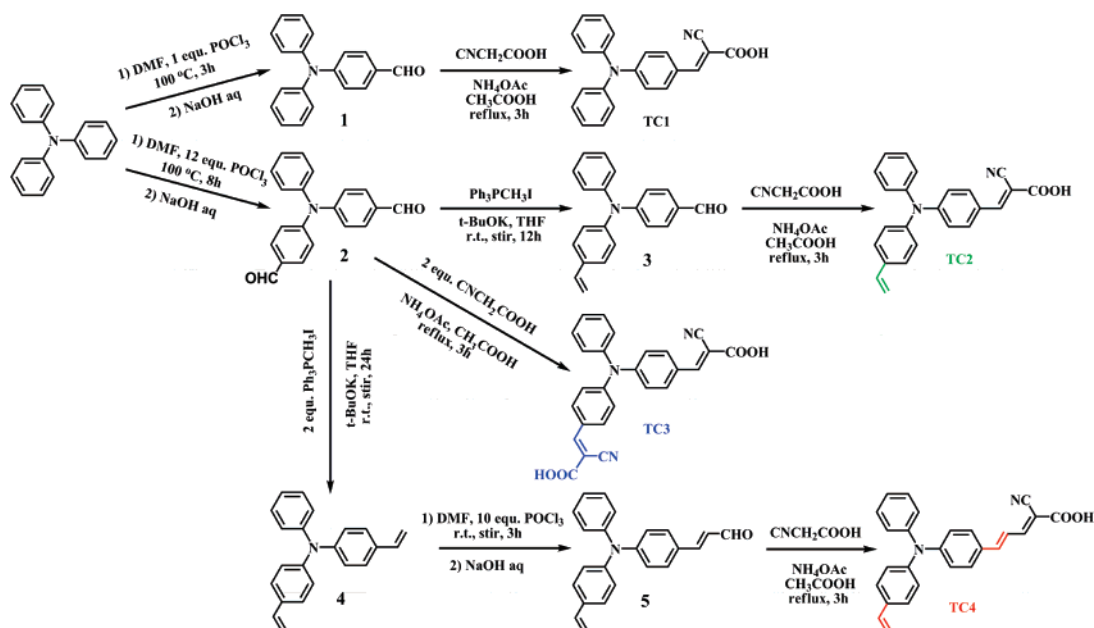
In this paper, we reported on the design, synthesis, and characterization of four metal-free organic donor-acceptor

dyes (Scheme 1) that contain donors with triphenylamine or its derivatives and cyano-acrylic acid acceptors bridged by a methine fragment. The TPA unit that is connected to the cyanoacrylic acid by a methine bridge is the basic model (TC1). To enhance the electron-donor ability of TPA, a vinyl unit was attached to the adjacent phenyl ring of TC1, leading to the structure of TC2. Introducing an acceptor moiety of cyanoacrylic acid to the adjacent phenyl ring of TC1 results in the structure of TC3. To extend the  $\pi$ -conjugated bridge, a methine unit was introduced to the bridge of TC2, producing TC4. The methine bridge takes the function as a photon sink where charge separation occurs, while the migration in the opposite direction is facilitated by the presence of donor and acceptor units. Theoretical calculation shows that electron-rich moiety in the donor and the bridge has a significant influence on the photoelectrochemical properties of the dyes. Experimental studies confirm that larger  $\pi$ -conjugated bridge and richer electron donor of the dyes are beneficial for the photovoltaic performance of the DSCs. In particular, TC4 exhibited the highest overall energy-conversion efficiency of 4.82% with a short-circuit photocurrent density of 11.5 mA/cm<sup>2</sup>, an open-circuit voltage of 652 mV, and a fill factor of 0.64 under irradiation with 100 mW/cm<sup>2</sup> simulated sunlight. The present results show that the as-synthesized metal-free organic dye photosensitizers are promising in the development of DSCs.

### Experiments and Calculations

**Materials and Reagents.** Potassium *tert*-butoxide, Triton X-100, and cyanoacetic acid were purchased from Fluka and Acros in analytical grade. All other solvents and chemicals used in this work were reagent grade (Tianjin Chemical Factory, China) and used without further purification. Tetrabutylammonium perchlorate (TBAP) and 1,2-dimethyl-3-propylimidazolium iodide (DMPImI) were synthesized and purified according

\* To whom correspondence should be addressed. Fax: +86-22-2350-9118. E-mail: chenabc@nankai.edu.cn.

SCHEME 1: Molecular Structures and Synthesis of the Triphenylamine-Based TC1, TC2, TC3, and TC4 Dyes<sup>a</sup>

<sup>a</sup> The difference between TC1 and TC2–TC4 has been marked by color drawings.

to the literature.<sup>27,28</sup> Transparent conducting oxide glass substrates (F-doped SnO<sub>2</sub> over layer with sheet resistance of 10 Ω/sq, Nippon Sheet Glass, Hyogo, Japan) were washed under supersonication for 15 min with Triton X-100, ethanol, and acetone, respectively. Commercial TiO<sub>2</sub> (P25, a mixture of 30% rutile and 70% anatase, Degussa AG, Germany) was used for the preparation of the nanocrystalline films.

**Spectroscopic Measurements.** <sup>1</sup>H nuclear magnetic resonance (NMR) spectra of the as-prepared dyes were carried out with a Varian Mercury Vx300 spectrometer at 300 MHz with the chemical shifts against tetramethylsilane (TMS). Electro-spray ionization mass spectrometry (ESI-MS) spectra were measured with a LCQ AD (ThermoFinnigan, USA) mass spectrometer. The absorption spectra of the dyes in solution and adsorbed on TiO<sub>2</sub> films were measured with a Jasco-550 UV/vis spectrophotometer. The fluorescence spectra of the dyes in methanol solution were observed on a Cary Eclipse fluorescence spectrophotometer at ambient temperature. Samples were contained in 1-cm path-length quartz cells.

**Synthetic Procedure of TC1–TC4.** TC1, TC2, TC3, and TC4 dyes were synthesized by well-known reactions such as Wittig reaction, Vilsmeier–Haack formylation reaction, and Knoevenagel reaction. The starting triphenylamine (TPA) was synthesized from phenylamine and iodobenzene in a nitrogen atmosphere (Cu catalyst, 115 °C, 3.5 h).<sup>29</sup> 4-(Diphenylamino)benzaldehyde and 4,4'-(phenylazanediyl)dibenzaldehyde were prepared by treating TPA with different equivalent of POCl<sub>3</sub> in DMF, according to literature procedures.<sup>30</sup> The detailed synthetic procedures of TC1, TC2, TC3, and TC4 were described as following.

**2-Cyano-3-(4-(diphenylamino)phenyl)acrylic Acid (TC1).** 4-(Diphenylamino)benzaldehyde (273 mg, 1 mmol) and 2-cyanoacetic acid (128 mg, 1.5 mmol) were added to 15 mL of glacial acetic acid and refluxed for 3 h in the presence of 150 mg of ammonium acetate. After cooling to room temperature, the mixture was poured into ice water. The precipitate was filtered, washed by distilled water, dried under vacuum, and purified by column chromatography (acetate/ethanol), resulting in yellow powder of TC1 (230 mg, 67.6%). <sup>1</sup>H NMR (300 MHz,

DMSO-*d*<sub>6</sub>) δ (ppm): 8.00 (s, 1H), 7.88 (d, 2H), 7.42 (t, 4H), 7.25–7.18 (m, 6H), 6.90 (d, 2H). ESI-MS: *m/z* 339 ([M – H]<sup>–</sup>).

**2-Cyano-3-(4-(phenyl(4-vinylphenyl)amino)phenyl)acrylic Acid (TC2).** Same as TC1 but 4-(phenyl(4-vinylphenyl)amino)benzaldehyde (300 mg, 1 mmol) instead of 4-(diphenylamino)benzaldehyde was used, resulting in yellow powder (240 mg, 65.6%). <sup>1</sup>H NMR (300 MHz, DMSO-*d*<sub>6</sub>) δ (ppm): 7.93 (s, 1H), 7.78 (d, 2H), 7.35 (t, 4H), 7.15–7.04 (m, 6H), 6.92 (t, 1H), 6.71 (dd, 1H), 5.80 (d, 1H), 5.25 (d, 1H). ESI-MS: *m/z* 365 ([M – H]<sup>–</sup>).

**3,3'-(4,4'-(Phenylazanediyl)bis(4,1-phenylene))bis(2-cyanoacrylic Acid) (TC3).** Same as TC1 but 4,4'-(phenylazanediyl)dibenzaldehyde (301 mg, 1 mmol) instead of 4-(diphenylamino)benzaldehyde and 2-cyanoacetic acid (256 mg, 3.0 mmol) was used. The isolated dark-yellow powder (305 mg, 70.1%) is TC3, showing <sup>1</sup>H NMR (300 MHz, DMSO-*d*<sub>6</sub>) δ (ppm): 8.05 (s, 2H), 7.95 (d, 4H), 7.46 (t, 2H), 7.29 (t, 1H), 7.24 (d, 2H), 7.14 (d, 4H). ESI-MS: *m/z* 434 ([M – H]<sup>–</sup>).

**2-Cyano-5-(4-(phenyl(4-vinylphenyl)amino)phenyl)penta-2,4-dienoic Acid (TC4).** Same as TC1 but 3-(4-(phenyl(4-vinylphenyl)amino)phenyl)acrylaldehyde (326 mg, 1 mmol) instead of 4-(diphenylamino)benzaldehyde was used. The isolated red powder (284 mg, 72.4%) is TC4, revealing <sup>1</sup>H NMR (300 MHz, DMSO-*d*<sub>6</sub>) δ (ppm): 7.78 (d, 1H), 7.50 (d, 2H), 7.44 (d, 2H), 7.35 (t, 2H), 7.29 (d, 1H), 7.18–6.99 (m, 7H), 6.91 (t, 1H), 6.70 (dd, 1H), 5.77 (d, 1H), 5.23 (d, 1H). ESI-MS: *m/z* 391 ([M – H]<sup>–</sup>).

**Electrochemical Measurements.** The oxidation potentials of the dyes in acetonitrile/acetic acid were measured in a normal one-compartment cell with a glassy carbon working electrode, a Pt wire counter electrode, and a Ag/Ag<sup>+</sup> reference electrode in an acetonitrile solution including 0.01 M AgNO<sub>3</sub> and 0.1 M TBAP. The potential of the reference electrode is 0.351 V vs a normal hydrogen electrode (NHE) and calibrated with ferrocene. The measurements were performed with a PARSTAT 2273 electrochemical analyzer. The supporting electrolyte was 0.1

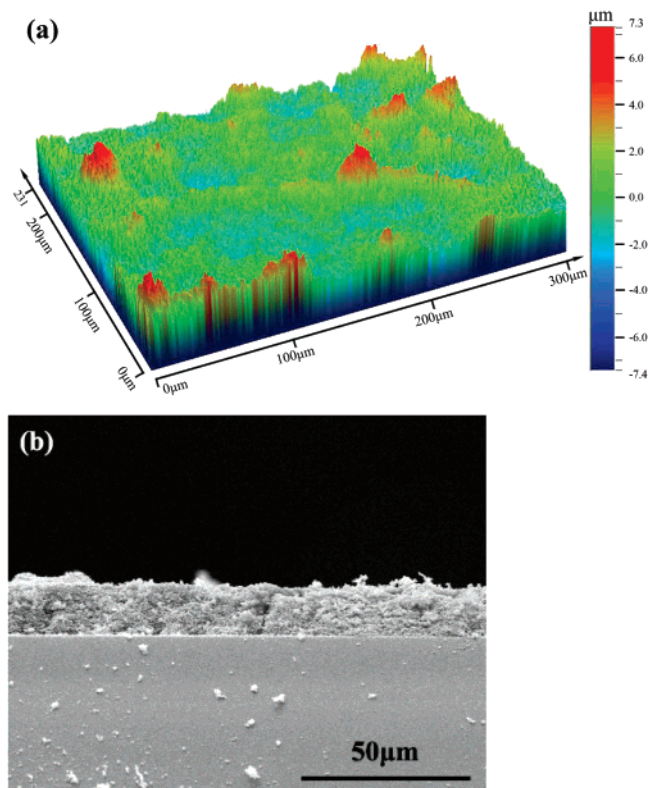


**Figure 1.** (a) Three-dimensional surface image and (b) cross-sectional SEM image of the as-prepared TiO<sub>2</sub> film coated on the conducting glass.

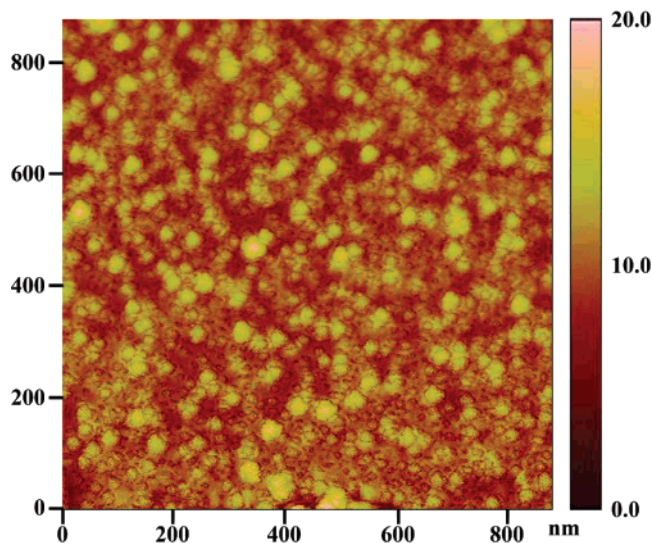


**Figure 2.** A representative tapping-mode AFM image of Pt counter electrode.

M TBAP in dry acetonitrile/acetic acid (7/1, v/v), which was purged with argon (99.999%) and stirred for 15 min prior to the scan.

**Computation Methods.** The geometrical and electronic properties of the compounds (TC1–TC4) were performed with the Gaussian 03 program package.<sup>31</sup> The calculation was optimized by means of the B3LYP (Becke three parameters hybrid functional with Lee–Yang–Perdew correlation functionals) with the Pople 6-31G(d,p) atomic basis set.<sup>32</sup> The excitation transitions of TC4 were calculated using time-dependent density functional theory (TD-DFT) calculations with B3LYP/6-31g(d,p). Molecular orbitals were visualized using Gaussview.

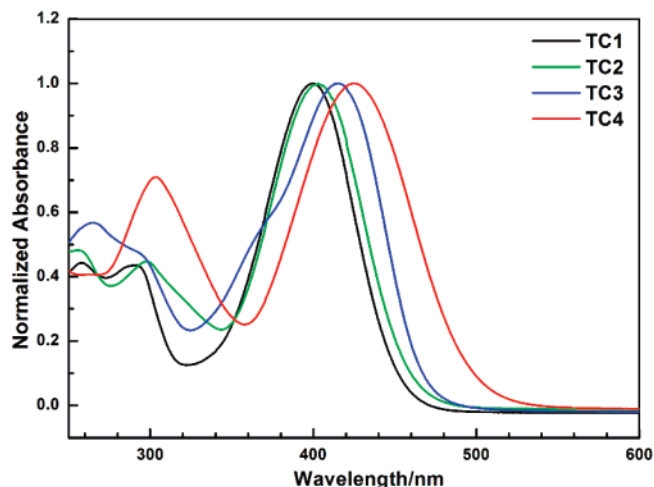


**Figure 3.** Normalized absorption spectra of the TC1, TC2, TC3, and TC4 measured in methanol solution.

**TABLE 1: The Fluorescence Emission Properties of TC1–TC4**

dye	$\lambda_{\max}^a/\text{nm}$	$\epsilon_{\max}^a/\text{M}^{-1} \text{cm}^{-1}$	$\lambda_{\text{em}}^b/\text{nm}$	amount <sup>c</sup> / $10^{-8} \text{mol cm}^{-2}$
TC1	400	15 800	554	11.9
TC2	403	29 300	542	14.9
TC3	416	18 600	548	9.9
TC4	425	26 900	585	7.1

<sup>a</sup> <sup>b</sup> Absorption and emission spectra were measured in methanol solution. The emission spectra were obtained with the concentration of  $5 \times 10^{-5} \text{ M}$  at 293 K.  $\epsilon_{\max}$  is the extinction coefficient at  $\lambda_{\max}$  of absorption. <sup>c</sup> Amount of the dyes adsorbed on TiO<sub>2</sub> film.

**Preparation of Dye-Adsorbed TiO<sub>2</sub> Films.** The TiO<sub>2</sub> paste, which consists of 16.2% P25 and 4.5% ethyl cellulose in terpineol, was printed on a conducting glass using a screen printing technique. The film was dried in air at 100 °C for 15 min followed by another 15 min at 150 °C. Then the film was calcined at 350 °C for 10 min. Finally the film was treated at 450 °C for 30 min under oxygen atmosphere. After cooling to room temperature, the electrodes were impregnated in 0.05 M titanium tetrachloride aqueous solution, washed with distilled water and recalcined at 450 °C for 30 min. The surface of the TiO<sub>2</sub> electrode was measured by a Microtek scanner with the image integration of 600 dpi resolution. The three-dimension (3D) surface image of the TiO<sub>2</sub> electrode was obtained by a Wyko NT1100 Optical Profiler (Veeco Metrology Group),<sup>33</sup> which was based on white-light scanning interferometry specific feature. As shown in Figure 1a, the porous and rough surface of the film with a peak-to-peak roughness of 14700 nm and a rms roughness of 1290 nm benefits the adsorption of the dyes, which results in the amount of the adsorbed dye around  $10^{-7} \text{ mol per square centimeter}$  discussed below. The thickness of the resulting films, measured by a Dektak 6M Stylus Profiler, was ca. 15  $\mu\text{m}$ , which was further confirmed by the cross section analysis of scanning electron microscopy (SEM) image of the film (Figure 1b) using a Philips XL-30 microscope.<sup>34</sup>

The TiO<sub>2</sub> electrodes were immersed into a dry methanol solution of the dye (standard concentration  $3 \times 10^{-4} \text{ M}$ ) and kept at room temperature for 24 h. The dye-coated electrodes were rinsed quickly with ethanol, and the photoelectrochemical measurement was conducted immediately.

**Fabrication of Dye-Sensitized Solar Cells.** The electrochemical cell used for photovoltaic measurements consisted of a dye-adsorbed TiO<sub>2</sub> electrode, a counter electrode, a tape spacer (42  $\mu\text{m}$  thick for the sealing), and an organic electrolyte. The electrolyte solution was a mixture of 0.6 M DMPImI, 0.1 M

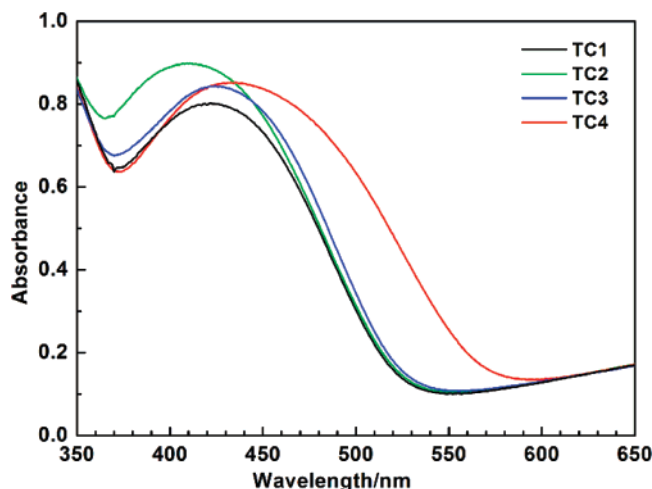


Figure 4. Absorption spectra of TiO<sub>2</sub> film with different sensitizers.

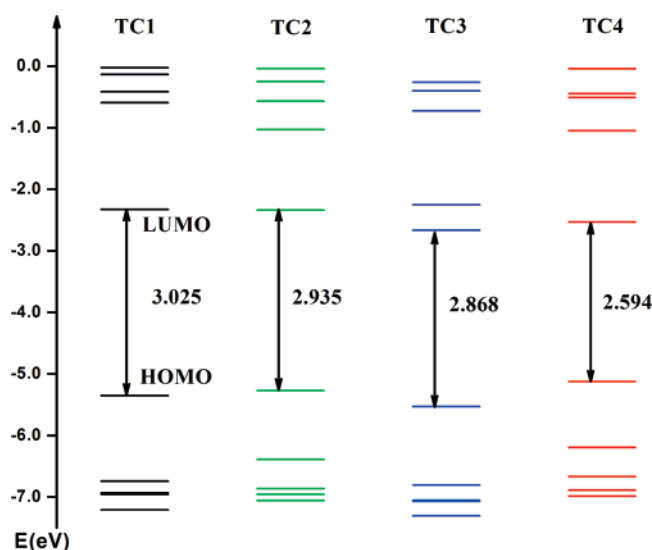


Figure 5. Schematic representation of the frontier molecular orbitals of TC1, TC2, TC3, and TC4 in methanol.

LiI, and 0.05 M I<sub>2</sub> in acetonitrile. As a counter electrode, a thin Pt layer was deposited on a FTO conducting glass by thermal pyrolysis of 30 mM H<sub>2</sub>PtCl<sub>6</sub> in isopropanol at 390 °C for 10 min.<sup>35</sup> The surface of the Pt film was imaged with a multimode Nano IIIa atomic force microscope (Veeco Metrology Group). An atomic force microscopy (AFM) height image of the as-prepared Pt thin film (Figure 2) reveals the homogeneous distribution of Pt nanoparticles with the character of smaller particles filled among the bigger particles, which are of great benefit to catalytic I<sub>3</sub><sup>-</sup> reduction.

**Photovoltaic Characterization.** Photoelectrochemical performance of the solar cell was measured using a Keithley 2400 digital source meter controlled by a computer.<sup>36</sup> A 500-W Xe lamp served as the light source in combination with a band-pass filter (400–800 nm) to remove ultraviolet and infrared radiation and to give 100 mW/cm<sup>2</sup> (the equivalent of one sun at AM1.5) at the surface of the test cell. The incident light intensity was calibrated by a radiometer. Further calibration was carried out by using a USB4000 plug-and-play miniature fiber optic spectrometer (Ocean Optics Inc., USA) to reduce the mismatch between the simulated and the true solar spectrum. The action spectra of monochromatic incident photo-to-current conversion efficiencies (IPCEs) for the solar cells were also detected with a similar data acquisition system. Light from a 500-W Xe lamp was focused through a monochromator onto

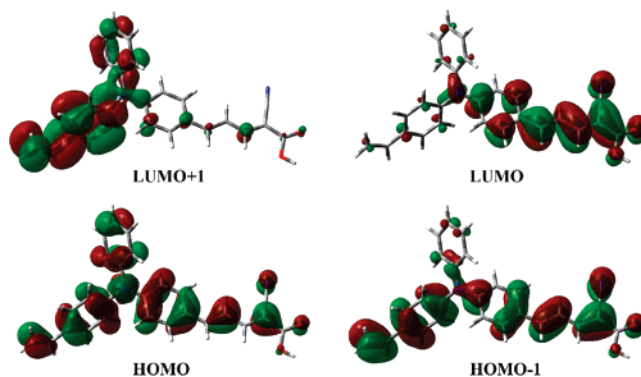


Figure 6. The frontier orbital plots of the HOMO-1, HOMO, LUMO, and LUMO+1 of TC4.

TABLE 2: Calculated TD-DFT Excitation Energies (*E*), Oscillator Strengths (*f*), and Composition in Terms of Molecular Orbital Contributions and Character, as Compared to the Maximum Band of Experimental Absorption (*n* Is the Ordering Number of the Calculated Excited State)

<i>n</i>	<i>E</i> (eV, nm)	<i>f</i>	composition	character	exptl (eV, nm)
1	2.34 (530)	1.10	85% HOMO → LUMO	CT	2.92 (425)
2	3.40 (365)	0.48	76% HOMO-1 → LUMO	π → π*	4.09 (303)
3	3.65 (340)	0.18	73% HOMO → LUMO+1	π → π*	
4	3.78 (328)	0.22	78% HOMO-2 → LUMO	π → π*	

the photovoltaic cell. The IPCE values were determined at 5 nm intervals according to eq (1)<sup>37</sup>

$$\text{IPCE } \% (\lambda) = \frac{1240 \text{ (eV} \cdot \text{nm)}}{\lambda \text{ (nm)}} \times \frac{J_{\text{sc}} \text{ (mA/cm}^2\text{)}}{\phi \text{ (mW/cm}^2\text{)}} \times 100 \quad (1)$$

where *J*<sub>sc</sub> is the short-circuit photocurrent density for monochromatic irradiation at wavelength *λ* and *Φ* is the power of the incident radiation per unit area. Light intensities were measured with a USB4000 Plug-and-Play Miniature Fiber Optic Spectrometer (Ocean Optics Inc., USA).

The solar energy-to-electricity conversion efficiency (*η*) of the DSCs is calculated from the short-circuit photocurrent density (*J*<sub>sc</sub>), the open-circuit photovoltage (*V*<sub>oc</sub>), the fill factor of the cell (*ff*), and the intensity of the incident light (*P*<sub>in</sub>) with eq (2)<sup>38</sup>

$$\eta \% = \frac{J_{\text{sc}} \text{ (mA/cm}^2\text{)} \times V_{\text{oc}} \text{ (V)} \times ff}{P_{\text{in}} \text{ (mW/cm}^2\text{)}} \times 100 \quad (2)$$

## Results and Discussion

**UV–Vis Absorption and Emission Spectra.** Figure 3 shows the absorption spectra of the as-synthesized dyes in methanol solution, with two distinct absorptions around 300 and 420 nm. The absorption band around 300 nm was assigned to a π–π\* transition, while the absorption band with *λ*<sub>max</sub> around 420 nm corresponded to an intramolecular charge transfer (ICT) between the TPA donor part of the molecule and the acceptor end group.<sup>39</sup> The spectrum of TC2 is quite similar to that of TC1 except for the broader absorption band at the short-wave region (<350 nm), which can be attributed to the introduction of vinyl (CH<sub>2</sub>=CH–) to adjacent phenyl ring. The absorption spectrum of TC3 (peak at 416 nm) was red-shifted in comparison with that of TC1 (400 nm) due to the acceptor moiety introduction of cyano-acrylic acid. Moreover, the spectrum of TC4 (peak at 425 nm) was obviously red-shifted in comparison with that of

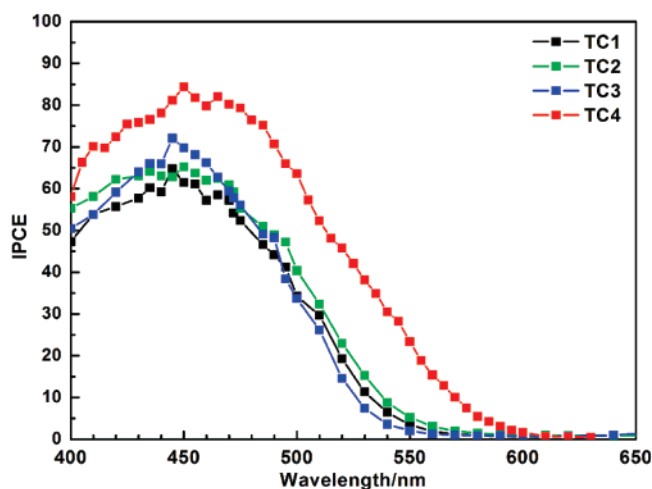


**Figure 7.** IPCE characteristics for DSCs based on the as-synthesized dyes. The redox electrolyte was comprised of 0.6 M DMPImI, 0.1 M LiI, and 0.05 M  $I_2$  in acetonitrile.

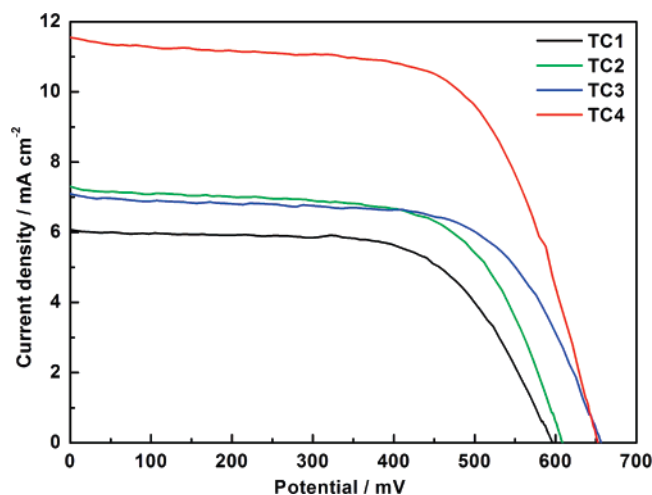


**Figure 8.** Current-voltage characteristics for the DSCs based on TC1, TC2, TC3, and TC4.

TC2 (403 nm) as well as stronger and broader around 300 nm, which is due to the expansion of  $\pi$ -conjugation systems by introducing the methine moiety into the  $\pi$ -bridge. Thus, the introduction of  $\pi$ -conjugated donor as well as acceptor part and expansion of the methine bridge contributed to a bathochromic shift in the absorption spectra of the dyes, which are desirable for harvesting the solar spectrum.

Table 1 summarizes the fluorescence emission properties of TC1, TC2, TC3, and TC4 in methanol solution. The wavelength of the emission peak was not strongly affected by modifying the donor part (554 nm for TC1 and 542 nm for TC2), but the peak was shifted toward the longer-wavelength region by expansion of the methine bridge (542 nm for TC2 and 585 nm for TC4).

Figure 4 shows the absorption spectrum of the four dyes adsorbed on a transparent  $TiO_2$  film. Compared to the spectrum in methanol solution, a red-shift and broadening of the absorption peak was observed in all dyes on  $TiO_2$  surface, which can be attributed to the formation of J-type aggregate.<sup>40</sup> The absorption before 370 nm belongs to  $TiO_2$  film and transparent glass. The amount of dyes adsorbed on the  $TiO_2$  films was estimated by desorbing the dye with basic solution, and the results are summarized in the right column of Table 1.

**TABLE 3: Electrochemical Data of the As-Synthesized Dyes<sup>a</sup>**

dye	$E_{0-0}$ /eV	$E(S^+/S)/V$ vs NHE	$E(S^+/S^*)/V$ vs NHE	$E_{gap}/V$
TC1	2.77	1.04	-1.73	1.23
TC2	2.80	1.08	-1.72	1.22
TC3	2.68	1.16	-1.52	1.02
TC4	2.53	0.96	-1.57	1.07

<sup>a</sup> The  $E_{0-0}$  value was estimated from the cross section of absorption and emission spectra. The redox potentials  $E(S^+/S)$  was measured on 0.1 M tetrabutylammonium perchlorate in acetonitrile using glassy carbon as the working electrode, Pt as the counter electrode, and  $Ag/Ag^+$  as the reference electrode, which was calibrated with ferrocene.<sup>47</sup> The excited state oxidation potential  $E(S^+/S^*)$  was calculated from  $E(S^+/S) - E_{0-0}$ .  $E_{gap}$  is the energy gap between the  $E(S^+/S^*)$  of the dye and the conduction band level of  $TiO_2$  (-0.5 V vs NHE).

**TABLE 4: Photovoltaic Performance of DSCs Based on the As-Synthesized (TC1–TC4) Dyes**

dye	$V_{oc}/mV$	$J_{sc}/mA\ cm^{-2}$	$ff$	$\eta/\%$
TC1	596	6.1	0.68	2.47
TC2	609	7.3	0.64	2.86
TC3	656	7.1	0.65	3.01
TC4	652	11.5	0.64	4.82

**Molecular Structure Analysis.** Figure 5 shows the schematic representation of the molecular orbital energies of TC1, TC2, TC3, and TC4. The electronic structure of the as-synthesized dyes was calculated in methanol solution that is the solvent used to record the experimental spectra. Observation of the frontier orbitals of the dyes except TC3 shows that the HOMO and LUMO are essentially isolated in energy, with the HOMO-1 below the HOMO and LUMO+1 above the LUMO both over 1.0 eV, respectively. The HOMO of TC3 is also isolated in energy, with the HOMO-1 lying 1.2 eV below its HOMO and the LUMO+1 lying 0.4 eV above the corresponding LUMO. This is owing to the influence of the two cyano-acrylic acid acceptors. In comparison, TC4 shows the narrowest HOMO-LUMO gap, which is beneficial for absorbing the long-wavelength light. Thus, TC4 is further chosen for the theoretical calculation, and the frontier orbitals of TC4 were depicted in Figure 6. The HOMO of TC4 is to a large extent delocalized over the entire molecule, indicating that the binding energy of the electron in the HOMO is sensitive to a change in the  $\pi$ -system.<sup>41</sup> Simultaneously, the LUMO of TC4 is a  $\pi^*$  orbital delocalized across the cyanoacrylic groups, and the LUMO+1 is a  $\pi^*$  orbital that is mainly delocalized over the styryl and the cyanoacrylic moiety.

To gain insight into the excited states of the dyes, we performed TD-DFT calculations of the lowest 10 singlet-singlet excitations of TC4 in methanol. By consideration of energy range, the four transitions with oscillator strengths ( $f$ ) above 0.1 are summarized in Table 2. The lowest transition is calculated to be 2.34 eV, corresponding to a charge-transfer excitation of the HOMO to the LUMO. The considerable red-shift of the absorption maximum from theory to experiments is related to the self-interaction error in TD-DFT arising through the electron transfer in the extended charge-transfer state.<sup>42</sup> The band experimentally found at 4.09 eV appears to be composed by three almost overlapping  $\pi$ - $\pi^*$  transitions of different character, calculated at 3.40, 3.65, and 3.78 eV. The three calculated transitions are  $\pi$ - $\pi^*$  transition from the HOMO-1 to the LUMO, the HOMO to the LUMO+1, and the HOMO-2 to the LUMO, respectively. The better agreement between the calculated and experimental absorption energies of the  $\pi$ - $\pi^*$  features as compared to the CT excitation is related to the

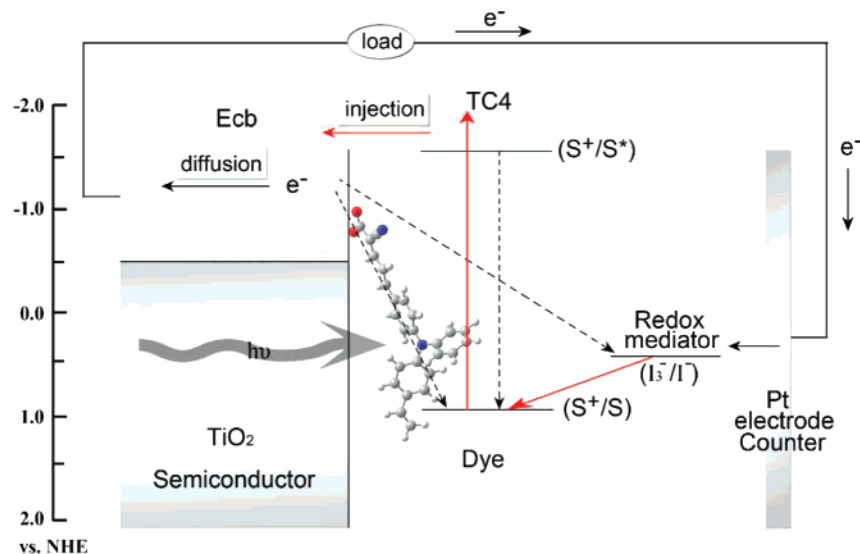


**Figure 9.** Schematic energy diagram for a DSC based on TC4 photosensitizer,  $I^-/I_3^-$  redox electrolyte,  $TiO_2$  anode, and Pt cathode.

localized character of the  $\pi-\pi^*$  excitations, which involve substantially overlapping orbitals.<sup>43</sup>

**Electrochemical Properties.** The formal redox potentials  $E(S^+/S)$  of the as-synthesized dyes were obtained by averaging the anodic and the cathodic peak potentials from cyclic voltammogram, and the results are summarized in Table 3. The oxidation potentials ranging from 0.96 to 1.16 V vs NHE are more positive than the  $I^-/I_3^-$  redox couple ( $\sim 0.4$  V vs NHE), ensuring that there is enough driving force for the dye regeneration efficiently through the recapture of the injected electrons from  $I^-$  by the dye cation radical. The redox potentials for TC1 and TC2 are 1.04 and 1.08 V (vs NHE), respectively, indicating that the introduction of ethenyl to the adjacent phenyl ring shifted the redox potential of the dyes in a positive direction. Meanwhile, introducing an electron-withdrawing 2-cyanoacrylic group ( $-\text{CH}=\text{C}(\text{CN})\text{COOH}$ ) into the framework of TC1 (producing TC3) resulted in a positive shift of 0.12 V (from 1.04 to 1.16 V). On the other hand, lengthening the methine unit of TC2 (producing TC4) shifted the redox potential of the dyes negatively (from 1.08 to 0.96 V).

Meanwhile, neglecting any entropy change during the light absorption, the excited-state oxidation potential  $E(S^+/S^*)$  can be extracted from the redox potential of the ground state  $E(S^+/S)$  and the zero-zero excitation energy  $E_{0-0}$  according to eq (3)<sup>44</sup>

$$E(S^+/S^*) = E(S^+/S) - E_{0-0} \quad (3)$$

From the data of Table 3, it can be seen that introducing ethenyl to adjacent phenyl ring of TC1 to form TC2 has little influence on  $E(S^+/S^*)$ . However, either introducing a 2-cyanoacrylic group into the framework of TC1 to the formation of TC3 or expanding the methine unit of TC2 to TC4 resulted in a positive shift in  $E(S^+/S^*)$ . The excited-state oxidation potentials of the four as-synthesized dyes (the data in the forth column of Table 3) are notably more negative than the equivalent potential of the  $TiO_2$  conduction band edge ( $-0.5$  V vs NHE), providing thermodynamic driving force for electron injection (1.02–1.23 V). By assumption that energy gap of 0.2 eV is necessary for efficient electron injection,<sup>45</sup> the present sensitizers could be very fascinating. In particular, for semiconductor materials that have Fermi levels more negative than that of titanium dioxide, an increased gap between the conduction band and the redox couple of electrolyte results in a higher open-circuit potential for improving the efficiency of DSCs.

**Photovoltaic Performance of DSCs.** Figure 7 shows the action spectra of monochromatic IPCEs for the sandwiched DSCs. The IPCE value of TC4-based DSC exceeds 70% in a spectral range from 410 to 490 nm and reaches its maximum of 84% at 450 nm. By consideration that the scattering and absorption losses in the transparent conducting-oxide substrate, the net photon-to-current conversion efficiency exceeds 90%. The IPCE spectrum of TC4-based DSC is red-shifted by about 35 nm as compared to that of the other dyes, which is consistent with its absorption spectra on a transparent  $TiO_2$  film. An interpretation of the best IPCE of TC4-based DSC follows. First, a large conjugated structure of TC4 dye makes electron transition much easier than that of the other dyes. Second, more delocalizing  $\pi$ -electrons on the conjugated donor moiety and the bridge part can generate more excited electrons under the same light excitation. This is beneficial for quantum yield of electron injection from dye molecule to semiconductor film, which is one of the important factors affecting the IPCE.<sup>46</sup> As a result, the DSC based on TC4 dye shows the best IPCE spectrum.

Figure 8 shows the  $I-V$  curves of DSCs based on the as-synthesized dyes. The detailed parameters ( $J_{sc}$ ,  $V_{oc}$ ,  $ff$ , and  $\eta$ ) are summarized in Table 4. The DSC based on TC4 dye shows a better comprehensive properties with an open circuit voltage of 652 mV, a short circuit photocurrent density of 11.5  $\text{mA cm}^{-2}$ , and a fill factor of 0.64, corresponding to an overall light to electricity conversion efficiency of 4.82% under AM 1.5 irradiation ( $100 \text{ mW cm}^{-2}$ ). The highest efficiency benefits from the highest short-circuit photocurrent density, which can be explained by the best IPCE value.

**Mechanism of Photon-to-Current Conversion in the DSCs.** Figure 9 shows the schematic energy diagram for a DSC based on TC4 photosensitizer. The HOMO and LUMO levels of the dye correspond to the formal redox potentials and the formal excited-state oxidation potential, respectively. The photon-to-current conversion involves the following primary processes. First, the dye is excited from the ground state to the excited state by the absorption of incident photon flux, owing to the intramolecular  $\pi-\pi^*$  transition. Second, the excited electron is injected into the conduction band of the  $TiO_2$  electrode immediately before quenching by emission and consequent formation of the oxidized dye. Third, the injected electrons in the conduction band of  $TiO_2$  are transported toward the Pt counter electrode through the external load. Fourth, the iodide is regenerated in turn by the reduction of triiodide at the Pt

counter electrode. Finally, the oxidized dyes reduce to the ground state by accepting electrons from the iodide anion that is oxidized to triiodide anion. It is thus that the reduction of both the oxidized dye and the triiodide determines the performance of a DSC.

## Conclusions

In this paper, we have successfully designed four metal-free organic dyes (TC1, TC2, TC3, and TC4) that contain donors with triphenylamine or its derivatives and cyano acrylic acid acceptors bridged by a methine fragment. The results based on experiment and computation show that extending the  $\pi$ -system of donor part and the bridge moieties appropriately can systematically control the spectral response of the dyes and further improve the energy conversion efficiency of DSCs. In particular, a maximum photo-to-electrical energy conversion efficiency of 4.82% was obtained with the DSC based on TC4 photosensitizer under AM 1.5 irradiation (100 mW cm<sup>-2</sup>), revealing that the as-synthesized metal-free organic dyes are promising in the development of DSCs. Work on dynamics of electron transport and recombination and the stability of DSCs based on the as-synthesized dyes are under study.

**Acknowledgment.** This work was supported by the National NSFC (20325102), 973 Program (2005CB623607) and TJKJ (05YFJMJC00300). We acknowledge the computational support by NKSTARS provided by the Center of Theoretical and Computational Chemistry at Nankai University.

## References and Notes

- (1) (a) O'Regan, B.; Grätzel, M. *Nature* **1991**, *353*, 737. (b) Grätzel, M. *Inorg. Chem.* **2005**, *44*, 6841.
- (2) (a) Park, N. G.; van de Lagemaat, J.; Frank, A. J. *J. Phys. Chem. B* **2000**, *104*, 8989. (b) Zhang, D. S.; Downing, J. A.; Knorr, F. J.; McHale, J. L. *J. Phys. Chem. B* **2006**, *110*, 21890.
- (3) Hauch, A.; Georg, A. *Electrochim. Acta* **2001**, *46*, 3457.
- (4) (a) Meng, Q. B.; Takahashi, K.; Zhang, X. T.; Sutanto, I.; Rao, T. N.; Sato, O.; Fujishima, A.; Watanabe, H.; Nakamori, T.; Urugami, M. *Langmuir* **2003**, *19*, 3572. (b) Kumar, R.; Sharma, A. K.; Parmar, V. S.; Watterson, A. C.; Chittibabu, K. G.; Kumar, J.; Samuelson, L. A. *Chem. Mater.* **2004**, *16*, 4841. (c) Shi, C. W.; Dai, S. Y.; Wang, K. J.; Pan, X.; Guo, L.; Zeng, L. Y.; Hu, L. H.; Kong, F. T. *Sol. Energy Mater. Sol. Cells* **2005**, *86*, 527.
- (5) Robertson, N. *Angew. Chem. Int. Ed.* **2006**, *45*, 2338.
- (6) <http://kuroppe.tagen.tohoku.ac.jp/~dsc/cell-e.htm>.
- (7) (a) Nazeeruddin, M. K.; Zakeeruddin, S. M.; Humphry-Baker, R.; Jirousek, M.; Liska, P.; Vlachopoulos, N.; Shklover, V.; Fischer, Christian-H.; Grätzel, M. *Inorg. Chem.* **1999**, *38*, 6298. (b) Nazeeruddin, M. K.; Péchy, P.; Renouard, T.; Zakeeruddin, S. M.; Humphry-Baker, R.; Comte, P.; Liska, P.; Cevey, L.; Costa, E.; Shklover, V.; Spiccia, L.; Deacon, G. B.; Bignozzi, C. A.; Grätzel, M. *J. Am. Chem. Soc.* **2001**, *123*, 1613.
- (8) (a) Hoertz, P. G.; Mallouk, T. E. *Inorg. Chem.* **2005**, *44*, 6828. (b) Meyer, G. J. *Inorg. Chem.* **2005**, *44*, 6852.
- (9) Sayama, K.; Tsukagoshi, S.; Hara, K.; Ohga, Y.; Shinpo, A.; Abe, Y.; Suga, S.; Arakawa, H. *J. Phys. Chem. B* **2002**, *106*, 1363.
- (10) Wang, Z. S.; Li, F. Y.; Huang, C. H.; Wang, L.; Wei, M.; Jin, L. P.; Li, N. Q. *J. Phys. Chem. B* **2000**, *104*, 9676.
- (11) Ehret, A.; Stuhl, L.; Spitler, M. T. *J. Phys. Chem. B* **2001**, *105*, 9960.
- (12) Hara, K.; Sato, T.; Katoh, R.; Furube, A.; Ohga, Y.; Shinpo, A.; Suga, S.; Sayama, K.; Sugihara, H.; Arakawa, H. *J. Phys. Chem. B* **2003**, *107*, 597.
- (13) Ferrere, S.; Gregg, B. A. *New J. Chem.* **2002**, *26*, 1155.
- (14) Ito, S.; Zakeeruddin, S. M.; Humphry-Baker, R.; Liska, P.; Charvet, R.; Comte, P.; Nazeeruddin, M. K.; Péchy, P.; Takata, M.; Miura, H.; Uchida, S.; Grätzel, M. *Adv. Mater.* **2006**, *18*, 1202.
- (15) Sayama, K.; Sugino, M.; Sugihara, H.; Abe, Y.; Arakawa, H. *Chem. Lett.* **1998**, *27*, 753.
- (16) Hara, K.; Kurashige, M.; Ito, S.; Shinpo, A.; Suga, S.; Sayama, K.; Arakawa, H. *Chem. Commun.* **2003**, 252.
- (17) Kim, Y. G.; Walker, J.; Samuelson, L. A.; Kumar, J. *Nano Lett.* **2003**, *3*, 523.
- (18) Hao, S. C.; Wu, J. H.; Huang, Y. F.; Lin, J. M. *Sol. Energy* **2006**, *80*, 209.
- (19) Satoh, N.; Cho, J. S.; Higuchi, M.; Yamamoto, K. *J. Am. Chem. Soc.* **2003**, *125*, 8104.
- (20) Satoh, N.; Nakashima, T.; Yamamoto, K. *J. Am. Chem. Soc.* **2005**, *127*, 13030.
- (21) Wang, Q.; Zakeeruddin, S. M.; Cremer, J.; Bäuerle, P.; Humphry-Baker, R.; Grätzel, M. *J. Am. Chem. Soc.* **2005**, *127*, 5706.
- (22) Bonhôte, P.; Moser, J.-E.; Humphry-Baker, R.; Vlachopoulos, N.; Zakeeruddin, S. M.; Walder, L.; Grätzel, M. *J. Am. Chem. Soc.* **1999**, *121*, 1324.
- (23) Kitamura, T.; Ikeda, M.; Shigaki, K.; Inoue, T.; Anderson, N. A.; Ai, X.; Lian, T. Q.; Yanagida, S. *Chem. Mater.* **2004**, *16*, 1806.
- (24) Velusamy, M.; Thomas, K. R. J.; Lin, J. T.; Hsu, Y. C.; Ho, K. C. *Org. Lett.* **2005**, *7*, 1899.
- (25) Hagberg D. P.; Edvinsson T.; Marinado T.; Boschloo G.; Hagfeldt A.; Sun L. C. *Chem. Commun.* **2006**, 2245.
- (26) Liang, M.; Xu, W.; Cai, F. S.; Chen, P.; Peng, B.; Chen, J.; Li, Z. M. *J. Phys. Chem. C* **2007**, *111*, 4465.
- (27) Jang, S. Y.; Seshadri, V.; Khil, M. S.; Kumar, A.; Marquez, M.; Mather, P. T.; Sotzing, G. A. *Adv. Mater.* **2005**, *17*, 2177.
- (28) Bonhôte, P.; Dias, A. P.; Papageorgiou, N.; Kalyanasundaram, K.; Grätzel, M. *Inorg. Chem.* **1996**, *35*, 1168.
- (29) Kelkar, A. A.; Patil, N. M.; Chaudhari, R. V. *Tetrahedron Lett.* **2002**, *43*, 7143.
- (30) Lai, G. F.; Bu, X. R.; Santos, J.; Mintz, E. A. *Synlett* **1997**, *11*, 1275.
- (31) Frisch, M. J.; Trucks, G. W.; Schlegel, H. B.; Scuseria, G. E.; Robb, M. A.; Cheeseman, J. R.; Montgomery, J. A., Jr.; Vreven, T.; Kudin, K. N.; Burant, J. C.; Millam, J. M.; Iyengar, S. S.; Tomasi, J.; Barone, V.; Mennucci, B.; Cossi, M.; Scalmani, G.; Rega, N.; Petersson, G. A.; Nakatsuji, H.; Hada, M.; Ehara, M.; Toyota, K.; Fukuda, R.; Hasegawa, J.; Ishida, M.; Nakajima, T.; Honda, Y.; Kitao, O.; Nakai, H.; Klene, M.; Li, X.; Knox, J. E.; Hratchian, H. P.; Cross, J. B.; Adamo, C.; Jaramillo, J.; Gomperts, R.; Stratmann, R. E.; Yazyev, O.; Austin, A. J.; Cammi, R.; Pomelli, C.; Ochterski, J. W.; Ayala, P. Y.; Morokuma, K.; Voth, G. A.; Salvador, P.; Dannenberg, J. J.; Zakrzewski, V. G.; Dapprich, S.; Daniels, A. D.; Strain, M. C.; Farkas, O.; Malick, D. K.; Rabuck, A. D.; Raghavachari, K.; Foresman, J. B.; Ortiz, J. V.; Cui, Q.; Baboul, A. G.; Clifford, S.; Cioslowski, J.; Stefanov, B. B.; Liu, G.; Liashenko, A.; Piskorz, P.; Komaromi, I.; Martin, R. L.; Fox, D. J.; Keith, T.; Al-Laham, M. A.; Peng, C. Y.; Nanayakkara, A.; Challacombe, M.; Gill, P. M. W.; Johnson, B.; Chen, W.; Wong, M. W.; Gonzalez, C.; Pople, J. A. *Gaussian 03*, revision C.01; Gaussian, Inc.: Wallingford, CT, 2004.
- (32) (a) Becke, A. D. *Phys. Rev. A* **1988**, *38*, 3098. (b) Lee, C.; Yang, W. T.; Parr, R. G. *Phys. Rev. B* **1988**, *37*, 785.
- (33) Tan, B.; Wu, Y. Y. *J. Phys. Chem. B* **2006**, *110*, 15932.
- (34) Gou, X. L.; Cheng, F. Y.; Shi, Y. H.; Zhang, L.; Peng, S. J.; Chen, J.; Shen, P. W. *J. Am. Chem. Soc.* **2006**, *128*, 7222.
- (35) Li, F. J.; Cheng, F. Y.; Shi, J. F.; Cai, F. S.; Liang, M.; Chen, J. *J. Power Sources* **2007**, *165*, 911.
- (36) Cai, F. S.; Chen, J.; Xu, R. S. *Chem. Lett.* **2006**, *35*, 1266.
- (37) Kamat, P. V.; Haria, M.; Hotchandani, S. *J. Phys. Chem. B* **2004**, *108*, 5166.
- (38) Hagfeldt, A.; Grätzel, M. *Acc. Chem. Res.* **2000**, *33*, 269.
- (39) Roquet, S.; Cravino, A.; Leriche, P.; Alévêque, O.; Frère, P.; Roncali, J. *J. Am. Chem. Soc.* **2006**, *128*, 3459.
- (40) Wang, Z. S.; Hara, K.; Dan-oh, Y.; Kasada, C.; Shinpo, A.; Suga, S.; Arakawa, H.; Sugihara, H. *J. Phys. Chem. B* **2005**, *109*, 3907.
- (41) Qin, P.; Yang, X.; Chen, R.; Sun, L.; Marinado, T.; Edvinsson, T.; Boschloo, G.; Hagfeldt, A. *J. Phys. Chem. C* **2007**, *111*, 1853.
- (42) Dreuw, A.; Head-Gordon, M. *J. Am. Chem. Soc.* **2004**, *126*, 4007.
- (43) Kim, S.; Lee, J. K.; Kang, S. O.; Ko, J.; Yum, J. H.; Fantacci, S.; Filippo, D. A.; Censo, D. D.; Nazeeruddin, M. K.; Grätzel, M. *J. Am. Chem. Soc.* **2006**, *128*, 16701.
- (44) Klein, C.; Nazeeruddin, K.; Liska, P.; Censo, D.; Hirata, N.; Palomares, E.; Durrant, J. R.; Grätzel, M. *Inorg. Chem.* **2005**, *44*, 178.
- (45) Hara, K.; Sato, T.; Katoh, R.; Furube, A.; Ohga, Y.; Shinpo, A.; Suga, S.; Sayama, K.; Sugihara, H.; Arakawa, H. *J. Phys. Chem. B* **2003**, *107*, 597.
- (46) Kalyanasundaram, K.; Grätzel, M. *Coord. Chem. Rev.* **1998**, *77*, 347.
- (47) Gagné, R. R.; Koval, C. A.; Lisensky, G. C. *Inorg. Chem.* **1980**, *19*, 2854.